

Supplement of Atmos. Chem. Phys. Discuss., 15, 2679–2744, 2015
<http://www.atmos-chem-phys-discuss.net/15/2679/2015/>
doi:10.5194/acpd-15-2679-2015-supplement
© Author(s) 2015. CC Attribution 3.0 License.



Supplement of

Secondary Organic Aerosol (SOA) formation from the β -pinene + NO₃ system: effect of humidity and peroxy radical fate

C. M. Boyd et al.

Correspondence to: N. L. Ng (ng@chbe.gatech.edu)

1 Formaldehyde needed for dry “RO₂+HO₂ dominant” Experiments

2 Formaldehyde is added to the chamber in order to enhance the RO₂+HO₂ chemistry. Without
3 formaldehyde injection, simulation results based on the Master Chemical Mechanism (Equations
4 are given at the end of Supplement) show that RO₂+RO₂ would be the dominant fate. However,
5 once sufficient formaldehyde is added to the chamber experiments, we determine that the
6 RO₂+HO₂ pathway is substantially greater than the RO₂+RO₂ pathway.

7
8 To determine the concentration of formaldehyde needed to favor the RO₂+HO₂ channel
9 significantly over the RO₂+RO₂ channel, a comparison of relative reaction rates is required.
10 Specifically, in order to favor a branching ratio of RO₂+HO₂ to RO₂+RO₂ by 95% (19:1), it is
11 necessary that

$$13 \quad k_{RO_2+HO_2}[HO_2][RO_2] = 19k_{RO_2+RO_2}[RO_2][RO_2] \quad (SR1)$$

$$14 \quad k_{RO_2+HO_2}[HO_2] = 19k_{RO_2+RO_2}[RO_2] \quad (SR2)$$

$$15 \quad k_{RO_2+HO_2} \frac{d[HO_2]}{dt} = 19k_{RO_2+RO_2} \frac{d[RO_2]}{dt} \quad (SR3)$$

16
17 Rates of production for each radical can then be used as a surrogate for the approximate
18 concentrations as the radicals are expected to be consumed immediately upon production. The
19 rates of production are:

$$21 \quad \frac{d[HO_2]}{dt} = k_{HCHO+NO_3}[HCHO][NO_3] \quad (SR4)$$

$$22 \quad \frac{d[RO_2]}{dt} = k_{\beta pin+NO_3}[\beta pin][NO_3] \quad (SR5)$$

23
24 Thus equation SR3 becomes:

$$26 \quad k_{RO_2+HO_2}k_{HCHO+NO_3}[HCHO][NO_3] = \quad (SR6)$$

$$27 \quad 19k_{RO_2+RO_2}k_{\beta pin+NO_3}[\beta pin][NO_3]$$

$$29 \quad k_{RO_2+HO_2}k_{HCHO+NO_3}[HCHO] = 19k_{RO_2+RO_2}k_{\beta pin+NO_3}[\beta pin] \quad (SR7)$$

30 Therefore, the ratio of formaldehyde to β -pinene should be ($k_{RO_2+RO_2} = 9.2E-14 \text{ cm}^3 \text{ molecules}^{-1}$
31 s^{-1} ; $k_{\beta\text{pin}+NO_3} = 2.5E-12 \text{ cm}^3 \text{ molecules}^{-1} \text{ s}^{-1}$; $k_{RO_2+HO_2} = 9.2E-14 \text{ cm}^3 \text{ molecules}^{-1} \text{ s}^{-1}$; $k_{HCHO+NO_3} =$
32 $5.5E-16 \text{ cm}^3 \text{ molecules}^{-1} \text{ s}^{-1}$, all rate constants are from MCM v3.2 (Saunders et al., 2003)):

$$34 \quad \frac{[HCHO]}{[\beta\text{pin}]} = \frac{19k_{RO_2+RO_2}k_{\beta\text{pin}+NO_3}}{k_{RO_2+HO_2}k_{HCHO+NO_3}} = 350 \quad (\text{SR8})$$

35

36 Results from Filter Sample Analysis

37 The UHPLC-MS total ion chromatogram for a typical “ RO_2+NO_3 dominant” experiment under
38 dry conditions is displayed in Fig. S4, which also represents the features observed in all other
39 experiments under dry and humid conditions. Excluding the solvent peak at ~ 0.2 min and
40 discarding the presence of any relevant species in the controls, the chromatogram in Fig. S4
41 reveals peaks with retention times of 3.26, 3.28, 6.19, 6.27, 7.03, and 7.08 min. These peaks are
42 displayed in the extracted ion chromatograms (EIC) for species with m/z 489, 244, 473, 489, 505
43 and 522.

44

45 The collisional induced dissociation (CID) of the peak at ~ 3.26 min is displayed in Fig. S5 for
46 the interval 30-70 V. Clearly, two anions with m/z 244 and 489 are observed at 3.26 min under
47 low fragmentation voltage (30 and 40 V). The prominent peak m/z 290 is mainly due the
48 presence of an adduct of the parent peak with formic acid: $[M-H] + HCOOH = 244 + 46 = 290$.
49 Support for the previous observation is also based on the appearance of the adduct $[M-H] +$
50 $CH_3COOH = 244 + 60 = 304$ in the presence of acetic acid, instead of formic acid, in the mobile
51 phase. The ion observed at m/z 197 becomes more intense at higher fragmentation voltage before
52 starting to break apart above 60 V. The parent peak m/z 244 must undergo the concerted loss of
53 nitrous acid, HNO_2 , to produce m/z 197. The loss of HNO_2 explains the change from an even to
54 an odd mass, which may be facilitated by intramolecular hydrogen transfer from the hydroxyl
55 group to the leaving $-NO_2$ moiety, leaving a carboxylate group as a rearranged fragment. The
56 confirmation of the presence of a $-COOH$ group in the neutral molecule with molecular mass
57 245 amu arises from the decarboxylative loss of 44 amu from the fragment ion m/z 197 that
58 generates a new fragment at m/z 153.

59

60 The MS peak at m/z 489 in Fig. S5 does not show the formation of either a formic acid or an
61 acetic acid adduct. In addition, the lack of a constant ratio for the ion count of species at m/z 244
62 and 489 in all experiments suggests that different formation pathways result in both products.
63 The careful analysis of the data presented showing the formation of formate or acetate adducts
64 for the species at m/z 244, and its excellent ionization at very low fragmentation voltage suggest
65 that the co-eluting species at m/z 489 should be a carboxylic acid molecule in the mechanistic
66 scheme (Fig. S6) to be presented below.

67
68 The chromatographic peak eluting at 6.19 min in Fig. S4 displayed as an EIC for m/z 505 with
69 broad features corresponds to a species with molecular weight (MW) of 506 amu. Given the
70 nitrogen rule, this species with even MW must contain an even number of nitrogen atoms. The
71 combination of two β -pinene molecules, which have incorporated nitrate radicals, provides a
72 starting mass of 396 amu for this species. The mass difference (506 – 396) amu = 110 amu
73 eliminates the possibility of including a third β -pinene molecule or two more nitrate radicals in
74 this product. Therefore, a general formula of $C_{20}H_{30}N_2O_{13}$ is assigned to this species. The ring
75 and double bond equivalency (RDB) defines the number of unsaturated bonds in the compound:

$$77 \quad RDB = 1 + \frac{\sum_i^{i_{max}} N_i(V_i - 2)}{2} \quad (SR17)$$

78
79 where i_{max} is the total number of different elements in the molecular formula, N_i is the number of
80 atoms of element i , and V_i is the valence of atom i (Pavia et al., 2008). For $C_{20}H_{30}N_2O_{13}$, RDB =
81 7 from limiting the calculated formulas that make sense chemically, a -C=O group should be
82 included in the structures of the mechanism forming species with this MW. Similarly, the EIC
83 for m/z 522 shows a broad peak that could correspond to a less polar isomer species eluting at
84 6.27 min. A molecular structure with two β -pinene units and an odd number of nitrogen atoms is
85 assigned to be $C_{20}H_{33}N_3O_{13}$ (MW = 523 amu) with RDB = 6 in the mechanism presented below.

86
87 Remarkably, a second species with m/z 489 elutes at 7.09 min in the EIC of Fig. S4, which
88 possesses a carbonyl group absorbing with $\lambda_{max} = 275$ nm in the UV-visible spectrum. This
89 molecule elutes later in the chromatogram, in the region of species with lower polarity –without
90 a -COOH group– because it corresponds to a less polar structural isomer than that eluting at 3.26

91 min. The most likely general formula for this species is $C_{20}H_{30}N_2O_{12}$ (MW = 490) with RDB = 7,
92 shown as the non-carboxylic acid structure in the mechanism introduced in the next section. A
93 slightly lighter species with m/z 473 (MW = 474 amu) and retention time of 7.03 min also
94 contains a carbonyl group in the UV-visible spectrum. The even molecular weight of this
95 molecule indicates a species with an even number of nitrogen atoms. The similar retention times
96 between both species (m/z 474 and 490) and the mass difference of only 16 amu suggests a
97 common molecular structure that differs by one oxygen atom. The molecular formula
98 $C_{20}H_{33}N_2O_{11}$ (MW = 474 amu) is represented by the proposed structures displayed in Fig. S6.

99

100 Figure S6 shows the further oxidation of some of the products shown in Fig. 8 of the main text.
101 Panel A of Fig. S6 shows the hydroxycarbonyl nitrate product with MW = 229 amu can be
102 further oxidized to the peroxy radical **V** by hydrogen abstraction from C_4 (R27) and subsequent
103 reaction with oxygen (R28). Hydrogen abstraction from the dihydroxycarbonyl nitrate generated
104 from **V** by R29 occurs preferentially on a $-CH_3$ group (C_9 or C_{10}) by R30, proceeding through an
105 alkyl radical with true trigonal pyramidal geometry, an unfavorable intermediate for C_5 , C_7 , and
106 C_8 due to the geometric constraints imposed by the cyclobutane ring (Vereecken and Peeters,
107 2012). Less likely is the abstraction occurring at C_4 , due to both the hindrance created by the
108 alcohol substituent and the slight strain from the adjacent butane ring. Addition of O_2 is also
109 included in R30 (Atkinson and Arey, 2003), resulting in a peroxy radical **W**. Reaction R31 for
110 $W + L'$ produces an alcohol ($R^{31}OH$) which can undergo a second H-abstraction by step 1 of
111 R32 at the same carbon, C_{10} . C_{10} is slightly more electropositive than C_9 due to the hydroxyl
112 substituent, and abstraction of the only H remaining at the more hindered C_4 of **W** is less likely
113 to occur than at C_{10} . Step 2 of R32 shows the formation of a peroxy radical **Y** through
114 combination with molecular oxygen (Atkinson and Arey, 2003). Panel B shows the oxidation of
115 the hydroxynitrate acid product, $R^{20}COOH$, through hydrogen abstraction and reaction with
116 molecular oxygen in R33 to peroxy radical **X**. Panel C shows in reaction R34 how a second
117 nitrate radical can add to the newly generated double bond of the hydroxynitrate product of R7
118 (Fig. 8, main text). The nitrate radical adds to the less substituted C_7 , leaving a relatively stable
119 tertiary alkyl radical on C_2 , which combines with O_2 via reaction R35 to form a peroxy radical **Z**.

120

121 Figure S7 shows how intermediates presented in Fig. 8 of the main text, **S**, **T**, and **U** combine
122 with radicals **V**, **W**, **X**, **Y**, **Z** presented in Fig. S6 to produce the heavier MW products observed
123 in aerosol filter extracts by UHPLC-MS via RO_2+RO_2 reactions. It is noted that each product in
124 Fig. S7 may be formed from the combination of other intermediates not explicitly drawn in Fig.
125 8 in the main text and Fig. S6. These findings are in agreement with previous work showing the
126 formation of organic peroxides during the oxidation of terpenes (Ng et al., 2008; Venkatachari
127 and Hopke, 2008; Docherty et al., 2005). Figure S7 shows that the major heavy MW species in
128 the UHPLC chromatogram of Fig. S4 can be generated from the same early oxidation
129 intermediates **S**, **T**, and **U**, implying the possible existence of more than one isomer for each
130 mass. The later observation is consistent with the EIC in Fig. S4 showing broad peaks in the
131 UHPLC-MS for m/z 505, 522, and the later 489, and a clear shoulder for m/z 473.

132

133 **Model Calculations for “ RO_2+NO_3 dominant” Experiments**

134 To ensure that the reaction conditions are favorable for the RO_2+NO_3 reaction, a simple chemical
135 model is developed using the Master Chemical Mechanism (MCM v3.2) as a basis (Saunders et
136 al., 2003). Reactions and their rate constants are shown in Table S1. The RO_2 fate in a typical
137 “ RO_2+NO_3 dominant” experiment (Experiment 5 in Table 1 of the main text) is shown in Fig.
138 S9.

139

140

141

142

143

144

145

146

147

148

149

150

151

152 **References**

153 Atkinson, R., and Arey, J.: Gas-phase Tropospheric Chemistry of Biogenic Volatile Organic
154 Compounds: A Review, *Atmos. Environ.*, 37, 197-219, 2003.

155
156 Docherty, K. S., Wu, W., Lim, Y. B., and Ziemann, P. J.: Contributions of Organic Peroxides to
157 Secondary Aerosol Formed from Reactions of Monoterpenes with O₃, *Environ. Sci. Technol.*,
158 39, 4049-4059, 2005.

159
160 Neuman, J. A., Nowak, J. B., Huey, L. G., Burkholder, J. B., Dibb, J. E., Holloway, J. S., Liao,
161 J., Peischl, J., Roberts, J. M., Ryerson, T. B., Scheuer, E., Stark, H., Stickel, R. E., Tanner, D. J.,
162 and Weinheimer, A.: Bromine measurements in ozone depleted air over the Arctic Ocean,
163 *Atmos. Chem. Phys.*, 10, 6503-6514, 10.5194/acp-10-6503-2010, 2010.

164
165 Ng, N. L., Kwan, A. J., Surratt, J. D., Chan, A. W. H., Chhabra, P. S., Sorooshian, A., Pye, H. O.
166 T., Crounse, J. D., Wennberg, P. O., and Flagan, R. C.: Secondary Organic Aerosol (SOA)
167 Formation from Reaction of Isoprene with Nitrate Radicals (NO₃), *Atmos. Chem. Phys.*, 8, 4117-
168 4140, 2008.

169
170 Odum, J. R., Hoffmann, T., Bowman, F., Collins, D., Flagan, R. C., and Seinfeld, J. H.:
171 Gas/Particle Partitioning and Secondary Organic Aerosol Yields, *Environ. Sci. Technol.*, 30,
172 2580-2585, 10.1021/es850943+, 1996.

173
174 Pavia, D., Lampman, G., Kriz, G., and Vyvyan, J.: Introduction to spectroscopy, Cengage
175 Learning, 2008.

176
177 Sander, S. P., Abbatt, J., Barker, J. R., Burkholder, J. B., Friedl, R. R., Golden, D. M., Huie, R.
178 E., Kolb, C. E., Kurylo, M. J., Moortgat, G. K., Orkin, V. L., and Wine, P. H.: Chemical kinetics
179 and photochemical data for use in atmospheric studies: Evaluation Number 17, Jet Propulsion
180 Laboratory, 2011.

181
182 Saunders, S. M., Jenkin, M. E., Derwent, R. G., and Pilling, M. J.: Protocol for the development
183 of the Master Chemical Mechanism, MCM v3 (Part A): tropospheric degradation of non-
184 aromatic volatile organic compounds, *Atmos. Chem. Phys.*, 3, 161-180, 2003.

185
186 Venkatachari, P., and Hopke, P. K.: Characterization of Products formed in the Reaction of
187 Ozone with α -pinene: Case for Organic Peroxides, *J. Environ. Monitor.*, 10, 966-974, 2008.

188
189 Vereecken, L., and Peeters, J.: A Theoretical Study of the OH-initiated Gas-phase Oxidation
190 Mechanism of β -pinene (C₁₀H₁₆): First Generation Products, *Phys. Chem. Chem. Phys.*, 14,
191 3802-3815, 10.1039/C2CP23711C, 2012.

192

193

194 **Table S1:** List of reactions and their rate constants for the β -pinene+NO₃ system. Reactions are
 195 adapted from MCMv3.2 (Saunders et al., 2003)^a.

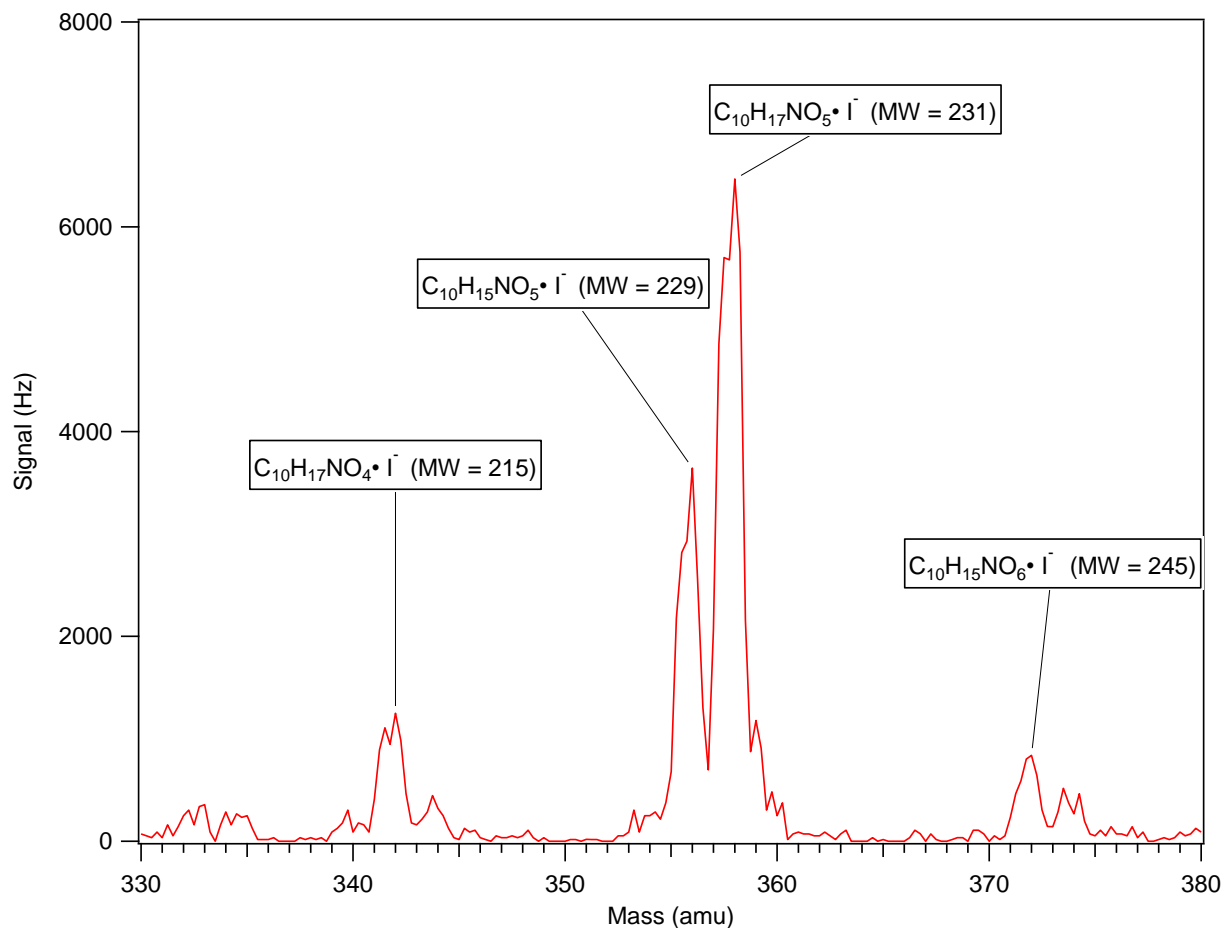
Reaction:	Rate Constant:
$\text{NO}_2 + \text{O}_3 \rightarrow \text{NO}_3 + \text{O}_2$	$3.2 \cdot 10^{-17} \text{ cc molecules}^{-1} \text{ s}^{-1\text{b}}$
$\text{NO}_2 + \text{NO}_3 \rightarrow \text{N}_2\text{O}_5$	$6.7 \cdot 10^{-12} \text{ cc molecules}^{-1} \text{ s}^{-1\text{b}}$
$\text{N}_2\text{O}_5 \rightarrow \text{NO}_2 + \text{NO}_3$	$2.2 \cdot 10^{-1} \text{ s}^{-1\text{b}}$
$\text{OH} + \text{O}_3 \rightarrow \text{HO}_2 + \text{O}_2$	$7.3 \cdot 10^{-14} \text{ cc molecules}^{-1} \text{ s}^{-1\text{b}}$
$\text{OH} + \text{HO}_2 \rightarrow \text{H}_2\text{O}_2 + \text{O}_2$	$1.1 \cdot 10^{-10} \text{ cc molecules}^{-1} \text{ s}^{-1\text{b}}$
$\text{HO}_2 + \text{O}_3 \rightarrow \text{OH} + 2\text{O}_2$	$1.9 \cdot 10^{-15} \text{ cc molecules}^{-1} \text{ s}^{-1\text{b}}$
$\text{HO}_2 + \text{HO}_2 \rightarrow \text{H}_2\text{O}_2 + \text{O}_2$	$1.4 \cdot 10^{-12} \text{ cc molecules}^{-1} \text{ s}^{-1\text{b}}$
$\text{NO} + \text{HO}_2 \rightarrow \text{NO}_2 + \text{OH}$	$8.1 \cdot 10^{-12} \text{ cc molecules}^{-1} \text{ s}^{-1\text{b}}$
$\text{NO} + \text{O}_3 \rightarrow \text{O}_2 + \text{NO}_2$	$1.9 \cdot 10^{-14} \text{ cc molecules}^{-1} \text{ s}^{-1\text{b}}$
$\text{NO} + \text{NO}_3 \rightarrow 2 \text{NO}_2$	$2.6 \cdot 10^{-11} \text{ cc molecules}^{-1} \text{ s}^{-1\text{b}}$
$\text{HCHO} + \text{NO}_3 \rightarrow \text{HNO}_3 + \text{CO} + \text{HO}_2$	$5.5 \cdot 10^{-16} \text{ cc molecules}^{-1} \text{ s}^{-1}$
$\beta\text{-pinene} + \text{NO}_3 + \text{O}_2 \rightarrow \text{NBPINAO}_2$	$0.8 \cdot 2.51 \cdot 10^{-12} \text{ cc molecules}^{-1} \text{ s}^{-1}$
$\beta\text{-pinene} + \text{NO}_3 + \text{O}_2 \rightarrow \text{NBPINBO}_2$	$0.2 \cdot 2.51 \cdot 10^{-17} \text{ cc molecules}^{-1} \text{ s}^{-1}$
$\beta\text{-pinene} + \text{O}_3 + \text{O}_2 \rightarrow \text{NOPINONE} + \text{CH}_2\text{OOF}$	$0.4 \cdot 1.5 \cdot 10^{-17} \text{ cc molecules}^{-1} \text{ s}^{-1}$
$\beta\text{-pinene} + \text{O}_3 + \text{O}_2 \rightarrow \text{NOPINOOA} + \text{HCHO}$	$0.6 \cdot 1.5 \cdot 10^{-17} \text{ cc molecules}^{-1} \text{ s}^{-1}$
$\text{NBPINAO}_2 + \text{HO}_2 \rightarrow \text{NBPINAOOH}$	$2.09 \cdot 10^{-11} \text{ cc molecules}^{-1} \text{ s}^{-1}$
$\text{NBPINAO}_2 + \text{NO} \rightarrow \text{NBPINAO}$	$9.04 \cdot 10^{-12} \text{ cc molecules}^{-1} \text{ s}^{-1}$
$\text{NBPINAO}_2 + \text{NO}_3 \rightarrow \text{NBPINAO}$	$2.3 \cdot 10^{-12} \text{ cc molecules}^{-1} \text{ s}^{-1}$
$\text{NBPINAO}_2 + \text{RO}_2 \rightarrow \text{NBPINAO}$	$0.7 \cdot 9.2 \cdot 10^{-14} \text{ cc molecules}^{-1} \text{ s}^{-1}$
$\text{NBPINAO} \rightarrow \text{NOPINONE} + \text{HCHO} + \text{NO}_2$	10^6 s^{-1}
$\text{NBPINAO}_2 + \text{RO}_2 \rightarrow \text{BPINBNO}_3$	$0.3 \cdot 9.2 \cdot 10^{-14} \text{ cc molecules}^{-1} \text{ s}^{-1}$
$\text{NBPINBO}_2 + \text{HO}_2 \rightarrow \text{NBPINBOOH}$	$2.09 \cdot 10^{-11} \text{ cc molecules}^{-1} \text{ s}^{-1}$
$\text{NBPINBO}_2 + \text{NO} \rightarrow \text{NBPINBO}$	$9.04 \cdot 10^{-12} \text{ cc molecules}^{-1} \text{ s}^{-1}$
$\text{NBPINBO}_2 + \text{NO}_3 \rightarrow \text{NBPINBO}$	$2.3 \cdot 10^{-12} \text{ cc molecules}^{-1} \text{ s}^{-1}$
$\text{NBPINBO}_2 + \text{RO}_2 \rightarrow \text{NBPINBO}$	$0.6 \cdot 2 \cdot 10^{-12} \text{ cc molecules}^{-1} \text{ s}^{-1}$
$\text{NBPINAO} \rightarrow \text{NOPINONE} + \text{HCHO} + \text{NO}_2$	$7 \cdot 10^3 \text{ s}^{-1}$
$\text{NBPINAO}_2 + \text{RO}_2 \rightarrow \text{BPINANNO}_3$	$0.2 \cdot 2 \cdot 10^{-12} \text{ cc molecules}^{-1} \text{ s}^{-1}$

$\text{NBPINAO}_2 + \text{RO}_2 \rightarrow \text{NC91CHO}$	$0.6 \cdot 2 \cdot 10^{-12} \text{ cc molecules}^{-1} \text{ s}^{-1}$
$\text{NC91CHO} + \text{NO}_3 \rightarrow \text{NC91CO}_3$	$2.32 \cdot 10^{-14} \text{ cc molecules}^{-1} \text{ s}^{-1}$
$\text{NC91CO}_3 + \text{HO}_2 \rightarrow \text{NC91CO}_3\text{H}$	$0.56 \cdot 1.39 \cdot 10^{-11} \text{ cc molecules}^{-1} \text{ s}^{-1}$
$\text{NC91CO}_3 + \text{HO}_2 \rightarrow \text{NOPINONE} + \text{NO}_3 + \text{OH} + \text{HCHO}$	$0.44 \cdot 1.39 \cdot 10^{-11} \text{ cc molecules}^{-1} \text{ s}^{-1}$
$\text{NC91CO}_3 + \text{NO} \rightarrow \text{NOPINONE} + \text{HCHO} + 2\text{NO}_2$	$1.98 \cdot 10^{-11} \text{ cc molecules}^{-1} \text{ s}^{-1}$
$\text{NC91CO}_3 + \text{NO}_2 \rightarrow \text{NC91PAN}$	$9.4 \cdot 10^{-12} \text{ cc molecules}^{-1} \text{ s}^{-1}$
$\text{NC91PAN} \rightarrow \text{NC91CO}_3 + \text{NO}_2$	$3.0 \cdot 10^{-4} \text{ s}^{-1}$
$\text{NC91CO}_3 + \text{NO}_3 \rightarrow \text{NOPINONE} + \text{HCHO} + 2\text{NO}_2$	$4.0 \cdot 10^{-12} \text{ cc molecules}^{-1} \text{ s}^{-1}$
$\text{NC91CO}_3 + \text{RO}_2 \rightarrow \text{NOPINONE} + \text{HCHO} + \text{NO}_2$	$10^{-11} \text{ cc molecules}^{-1} \text{ s}^{-1}$
$\text{CH}_2\text{OOFA} \rightarrow \text{CH}_2\text{OO}$	$0.37 \cdot 10^6 \text{ s}^{-1}$
$\text{CH}_2\text{OOFA} \rightarrow \text{CO}$	$0.5 \cdot 10^6 \text{ s}^{-1}$
$\text{CH}_2\text{OOFA} \rightarrow \text{HO}_2 + \text{CO} + \text{OH}$	$0.13 \cdot 10^6 \text{ s}^{-1}$
$\text{CH}_2\text{OO} + \text{CO} \rightarrow \text{HCHO}$	$1.2 \cdot 10^{-15} \text{ cc molecules}^{-1} \text{ s}^{-1}$
$\text{CH}_2\text{OO} + \text{NO} \rightarrow \text{HCHO}$	$1.0 \cdot 10^{-14} \text{ cc molecules}^{-1} \text{ s}^{-1}$
$\text{CH}_2\text{OO} + \text{NO}_2 \rightarrow \text{HCHO}$	$1.0 \cdot 10^{-15} \text{ cc molecules}^{-1} \text{ s}^{-1}$
$\text{CH}_2\text{OO} + \text{H}_2\text{O} \rightarrow \text{HCHO}$	$6.0 \cdot 10^{-18} \text{ cc molecules}^{-1} \text{ s}^{-1}$
$\text{CH}_2\text{OO} + \text{H}_2\text{O} \rightarrow \text{HCOOH}$	$1.0 \cdot 10^{-17} \text{ cc molecules}^{-1} \text{ s}^{-1}$

196 ^aUnless otherwise noted, all reaction rates are from MCM v. 3.2

197 ^bReaction rates are from Sander et al. (2011) and the references therein

198
199
200
201
202
203
204
205
206
207
208
209



210

211

212 **Figure S1:** Chemical Ionization Mass Spectrometry (CIMS) spectra for a typical “RO₂+HO₂
 213 dominant” experiment under dry conditions showing the major gas-phase compounds from the β-
 214 pinene+NO₃ reaction. The measured species are proposed to be organic nitrates due to their odd
 215 molecular weights. The specific molecular formulas for the ions shown are inferred from the
 216 chemical mechanism (Fig. 8, main text).

217

218

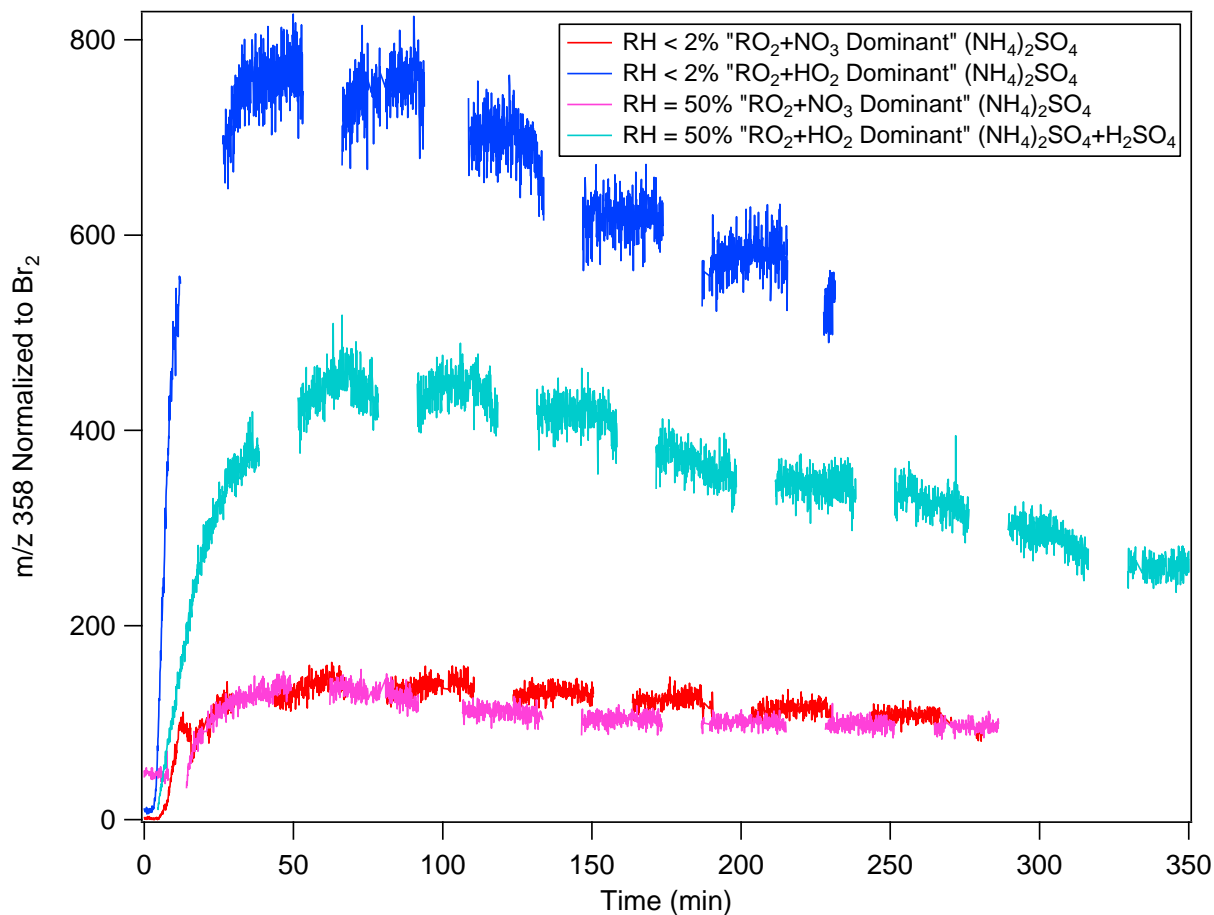
219

220

221

222

223

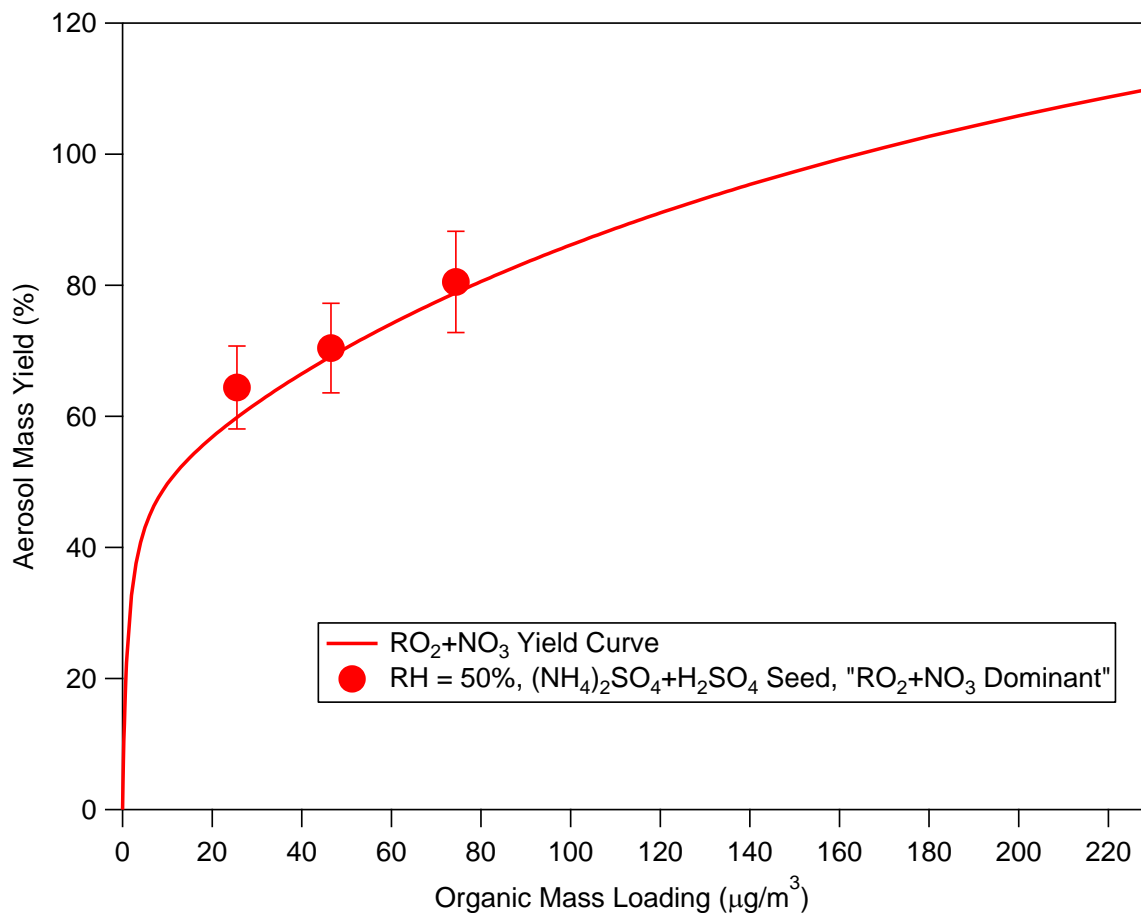


224

225

226 **Figure S2:** CIMS time series for m/z 358 for the β -pinene+NO₃ reaction at all conditions. m/z
 227 358 corresponds to a molecule-iodide adduct where the molecule has a molecular weight of 231
 228 amu. The signal is normalized to the instrument sensitivity to Br₂ to account for any sensitivity
 229 changes in the CIMS (Neuman et al., 2010). The species at m/z 358 is proposed to be either from
 230 a hydroperoxide (ROOH) or a dihydroxynitrate. It is significantly higher in experiments where
 231 RO₂+HO₂ is the dominant reaction pathway. Gaps in the data are from periodic measurements of
 232 the CIMS background. It is noted that the data shown above have not been corrected for CIMS
 233 background.

234



235

236

237 **Figure S3:** The yields for the experiments using $(\text{NH}_4)_2\text{SO}_4+\text{H}_2\text{SO}_4$ seed (circles) reported
 238 alongside the yields for the experiments using $(\text{NH}_4)_2\text{SO}_4$ seed (red curve) in “ RO_2+NO_3
 239 dominant” experiments. As seen in this figure, results from the experiments with
 240 $(\text{NH}_4)_2\text{SO}_4+\text{H}_2\text{SO}_4$ seed are in agreement with the yield curve generated by the two-product
 241 model (Odum et al., 1996) for experiments conducted in the presence of $(\text{NH}_4)_2\text{SO}_4$ seed.

242

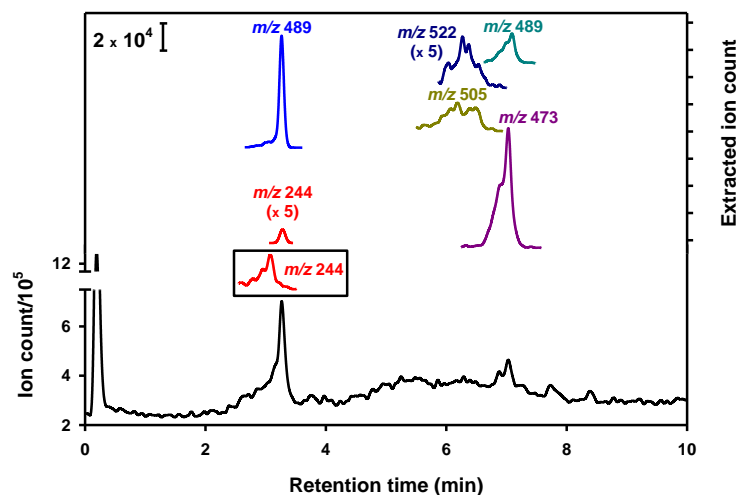
243

244

245

246

247



248

249

250 **Figure S4:** Total (bottom panel and left axis) and extracted (top panel and right axis) ion
 251 chromatogram (EIC) for eluting peaks at m/z 244, 489, 505, 522, and 473, and 489 in the
 252 UHPLC-MS chromatogram of a “ RO_2+NO_3 dominant” experiment under dry conditions, in the
 253 presence of 0.1 mM $HCOOH$ (fragmentor voltage = 50 v). The box shows the EIC for m/z 244
 254 using 0.4 mM CH_3COOH instead of $HCOOH$ (fragmentor voltage = 30 v).

255

256

257

258

259

260

261

262

263

264

265

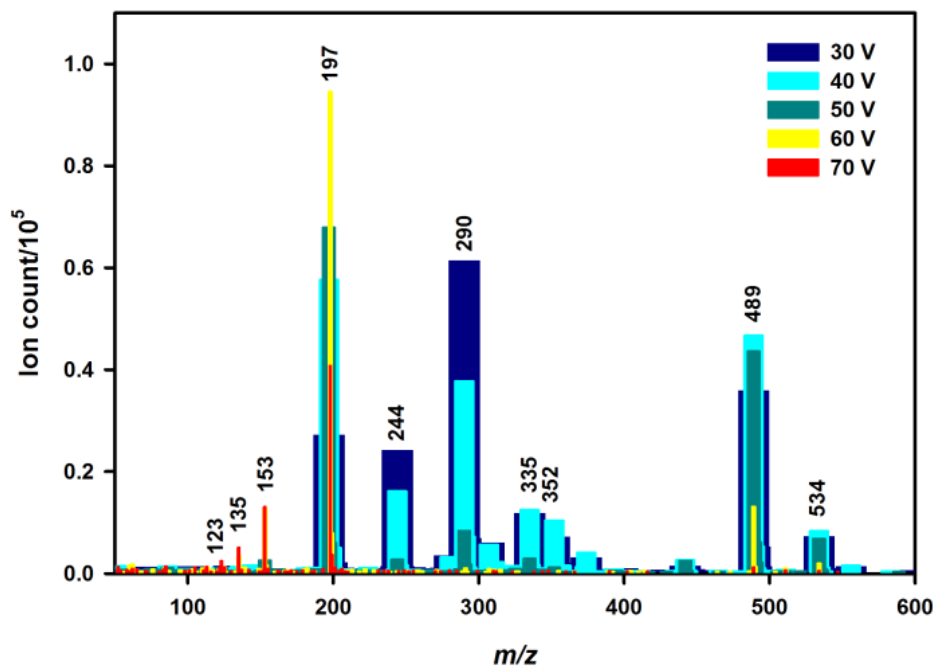
266

267

268

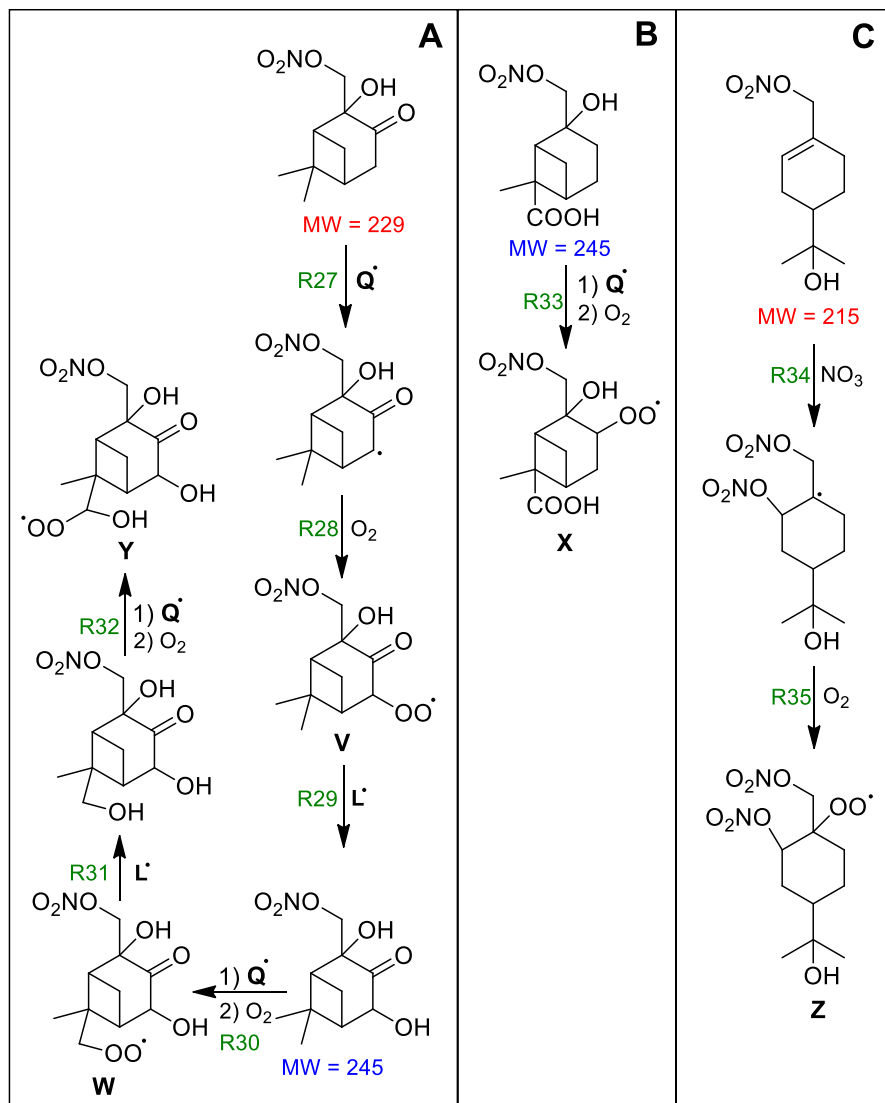
269

270



271
 272 **Figure S5:** Collisional induced dissociation mass spectra of chromatographic peak in Fig. S4 at
 273 3.27 ± 0.03 min between 30 and 70 V.

274
 275
 276
 277
 278
 279
 280
 281
 282
 283
 284
 285
 286
 287



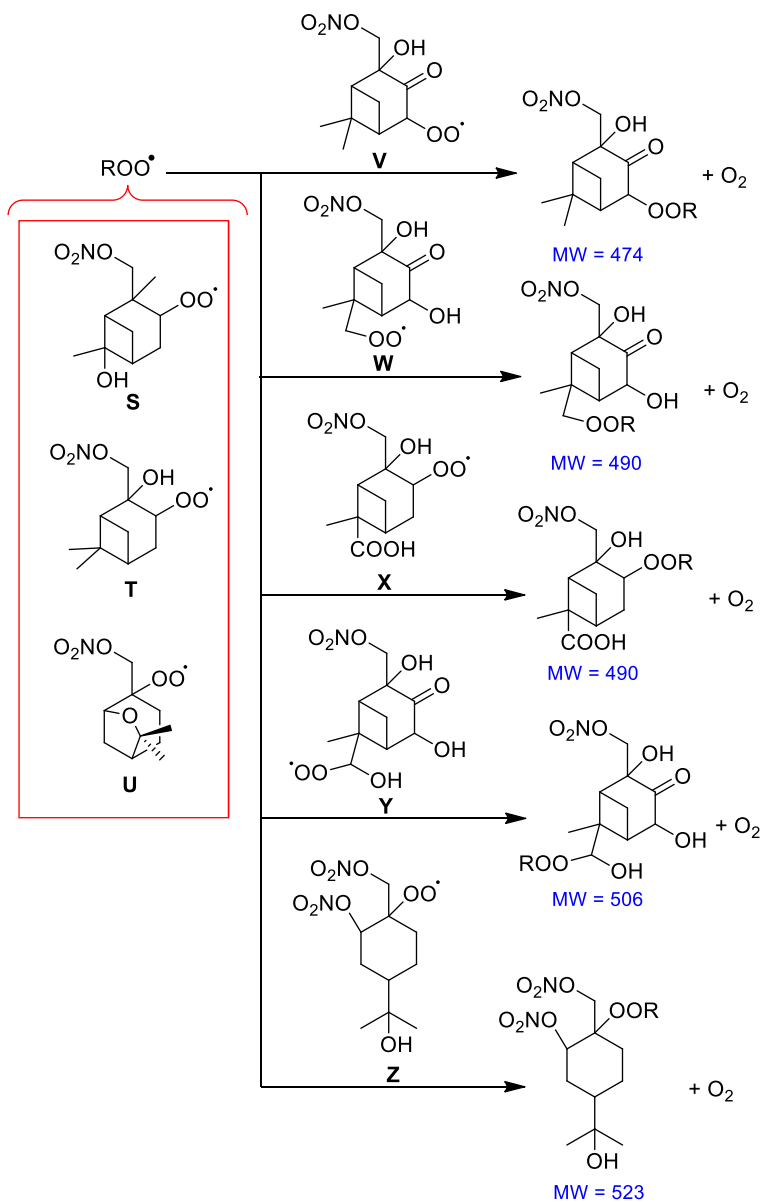
288

289

290 **Figure S6:** Proposed pathways for the further oxidation of products proposed in Fig. 8 of the
 291 main text. Named radicals are proposed to react to form the higher molecular weight species in
 292 Fig. S7.

293

294



295

296

297 **Figure S7:** Proposed pathways for the production of organic peroxides from radicals **S**, **T**, and **U**

298 (Fig. 8, main text) by reaction with radicals **V**, **W**, **X**, **Y**, and **Z** (Fig. S6, Supplement).

299

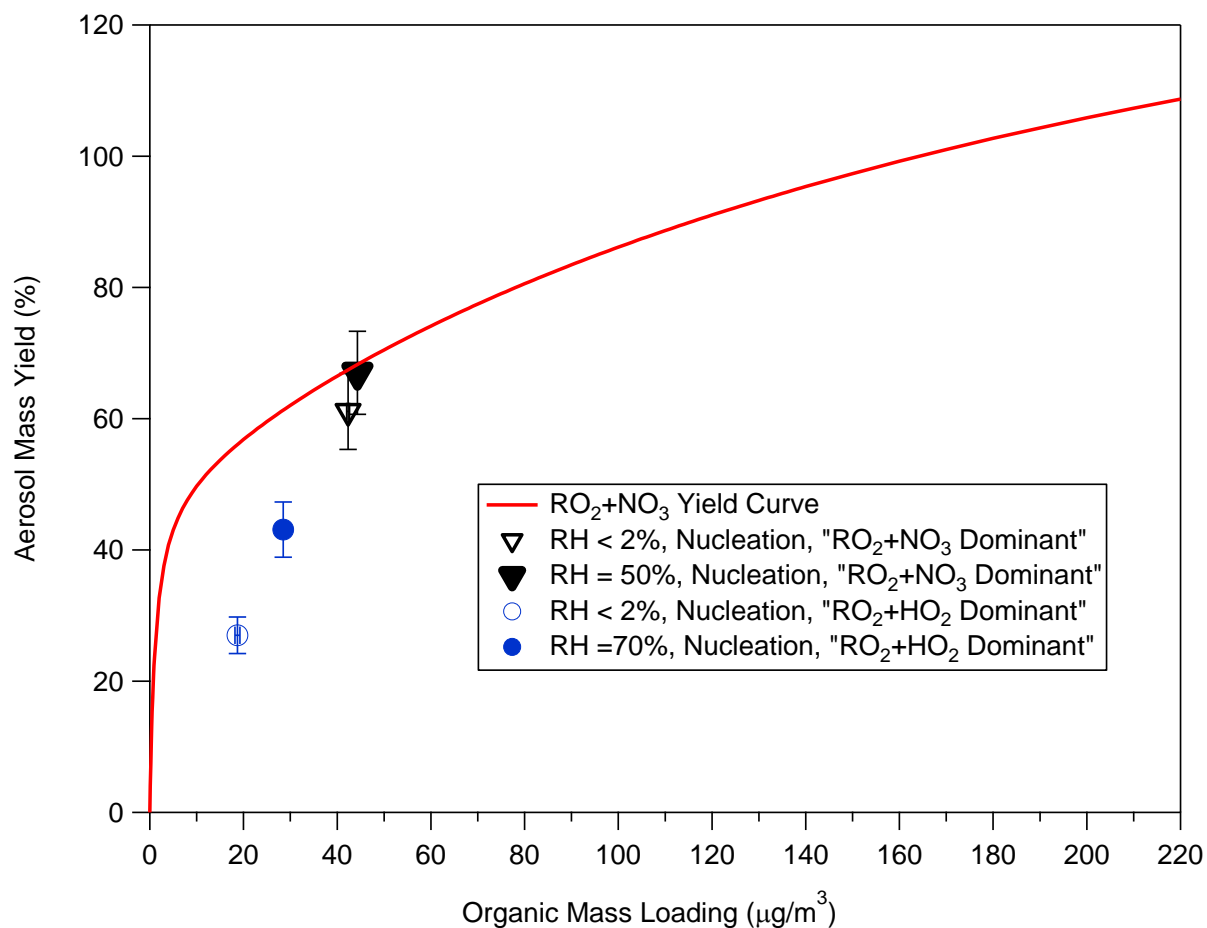
300

301

302

303

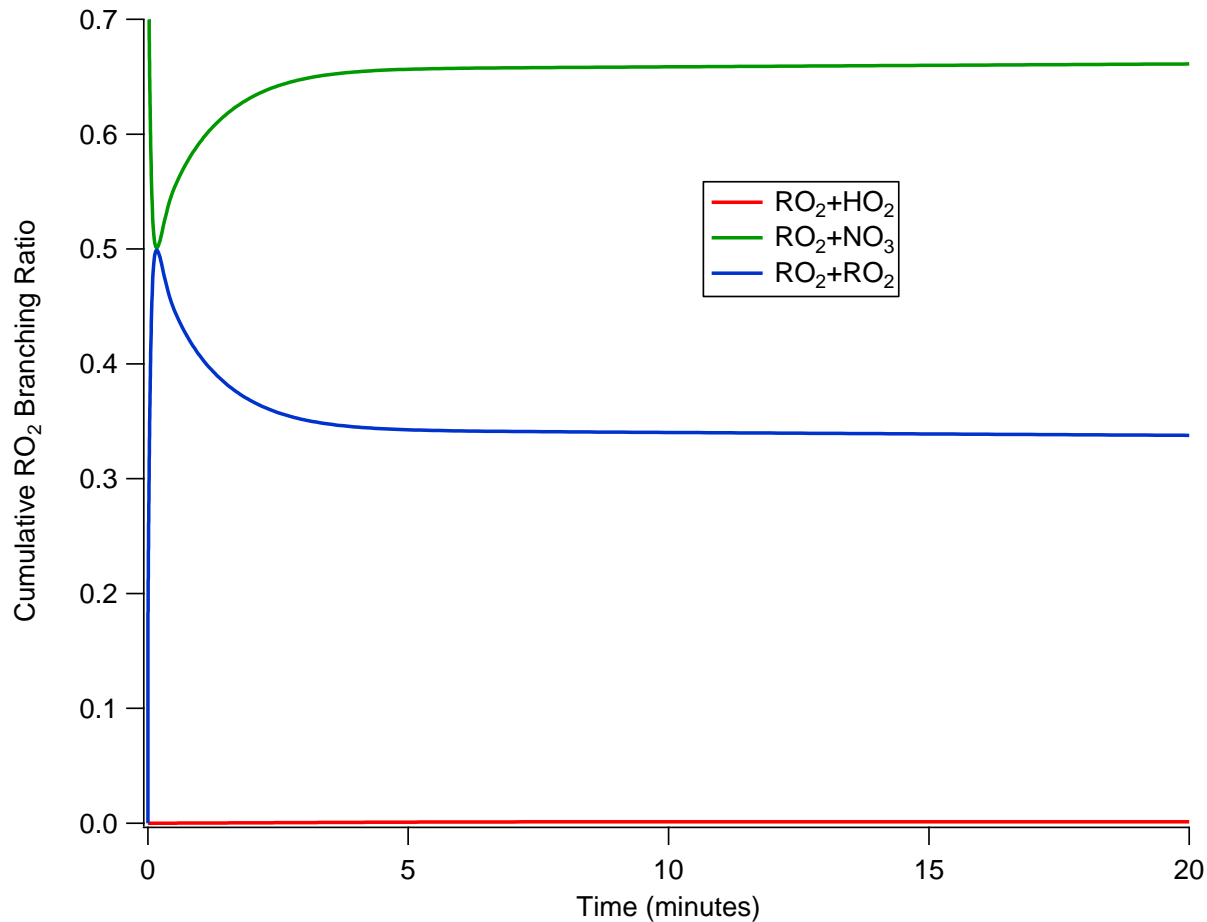
304



305
 306 **Figure S8:** The yields for nucleation experiments for all conditions are reported alongside the
 307 yields for experiments with (NH₄)₂SO₄ seed. The yields from the nucleation and seeded
 308 experiments in the “RO₂+NO₃ dominant” experiments are in agreement with each other while
 309 the “RO₂+HO₂ dominant” experiments are significantly lower than under seeded conditions. The
 310 y-axis error bars represent uncertainty in yield calculated by an 8% uncertainty in chamber
 311 volume, 5% uncertainty in hydrocarbon injection, and one standard deviation of the aerosol
 312 volume measured by SMPS at peak growth.

313
 314
 315
 316
 317
 318
 319

320



321

322

323 **Figure S9:** The RO₂ branching ratio for a typical “RO₂+NO₃” dominant experiment (Experiment
324 5 in Table 1 of the main text). The branching ratio is determined from the reactions in the Master
325 Chemical Mechanism (MCM v 3.2). The plot shows the cumulative amount of products formed
326 from each possible fate of RO₂ radicals.

327